

## High Frequency Switched Phase Controlled DC-AC Inverter

Bahadır ELMAS<sup>1\*</sup>, İzzet ALAGÖZ<sup>2</sup>,

<sup>1</sup> Mimar Sinan Güzel Sanatlar Üniversitesi, Fen Edebiyat Fakültesi, İstatistik Bölümü, 34380, İstanbul

<sup>2</sup> Elektrik Üretim Anonim Şirketi Genel Müdürlüğü, Genel Müdürlük, Ankara, 06520, Türkiye

Geliş / Received: 12/12/2020 Kabul / Accepted: 02/10/2021

### Abstract

With the increased power to weight ratio, corresponding to the developments in technology and material science, the demand for small uninterruptible power supply and high frequency transformers in transport vehicles and device technologies where the weight is particularly important has increased. An analysis of the high frequency switched phase-controlled DC-AC inverter and the high frequency transformer is presented. This inverter has a pair of switches in each side of the primary and the secondary of the transformer. The voltage conversion ratio is controlled by the phase difference between the two pairs of switches. The transformer is miniaturized by increasing the switching frequency. Thus the volume and weight of the system have been reduced. Current and voltage jumps in similar studies were reduced by using faster elements and opto-coupler, and these jumps were minimized by using snubber circuits. This DC-AC inverter and the high frequency transformers is especially suitable for small uninterruptible power supply systems. The circuit performed in the application is a 110 W DC-AC converter, the output voltage is 220 V, the efficiency is 93%. The high frequency transformer used in the application circuit has a physical size of 1/7 and a weight of 1/10 according to the sheet metal core transformer. When the circuit's power supply, driving circuits, switches, fans and filters were taken into consideration, its physical size was reduced by 1/5 and its weight by 2/3.

**Keywords:** DC-AC inverter, high frequency, transformer with ferrite core, phase controlled inverter, the voltage conversion ratio.

## Yüksek Frekans Anahtarlama Faz Kontrollü DC-AC İnvörtör

### Öz

Teknoloji ve malzeme bilimindeki gelişmelere paralel olarak artan güç-boyut oranı ile özellikle ağırlığın önemli olduğu ulaşım araçları ve cihaz teknolojilerinde küçük boyutlu kesintisiz güç kaynağı ve yüksek frekans transformatörlerine olan talep artış göstermektedir. Bu çalışmada, yüksek frekans anahtarlama faz kontrollü DC-AC invörtörler ve yüksek frekans transformatörleri incelenmiştir. Devredeki, transformatörünün primer ve sekonderinde birer çift anahtar bulunur. Gerilim transfer oranı, iki çift anahtar arasındaki faz farkı ile kontrol edilir. Anahtarlama frekansı yükseltilerek transformatör küçültülmüştür. Böylece sistemin hacmi ve ağırlığı azaltılmıştır. Benzer çalışmalardaki akım ve gerilim sıçramaları daha hızlı elamanlar ve opto-coupler kullanılarak azaltılmış, snubber devreleri kullanılarak bu sıçramalar minimuma çekilmiştir. Bu yapıdaki DC-AC invörtörler ve yüksek frekans transformatörleri özellikle küçük boyutlu kesintisiz güç kaynağı yapımı için uygundur. Uygulamada gerçekleştirilen devre 110 W'lık bir DC-AC dönüştürücü olup çıkış gerilimi 220 V, verimi %93'dür. Uygulama devresinde kullanılan yüksek frekans transformatörü, sac levha çekirdekli transformatöre göre fiziksel boyutu 1/7, ağırlığı 1/10'dur. Devrenin güç kaynağı, sürüş devreleri, anahtarlar, fanlar ve filtreler dikkate alındığında, fiziksel boyutu 1/5, ağırlığı 2/3 oranında azaltılmıştır.

**Anahtar Kelimeler:** DC-AC invörtör, yüksek frekans, ferrite çekirdekli transformatör, faz kontrollü invörtör, gerilim transfer oranı.

## **1. Introduction**

Uninterruptible power supply is a type of power supply system that contains a battery to maintain power to provide power to electronics in the event of a power surge or outage. The uninterruptible power supply may be three-phase or single-phase. They are divided into two general groups as dynamic and static. In addition, depending on whether the uninterruptible power supply operates continuously or not; on-line and off-line, according to the connection to the network; It is divided into two, directly connected and without connection (Bodur, 2011; Itoh et al., 2014).

Inverters are DC-AC converters that convert direct current into alternating current. Inverters are divided into two groups as voltage-fed and current-fed. When voltage-fed inverters are supplied with constant DC voltage, the current-fed inverters are supplied by a current source. In general, a single-phase voltage or current-Fed inverter; it may be in a push-pull connection with half bridge, H-bridge or midpoint transformer. Single-phase inverters are connected to each other three-phase or multiphase AC systems can be obtained (Bodur, 2011). The high gain DC-AC converters are widely used in various applications such as employed for battery, solar photovoltaic, fuel cell fed applications like domestic lighting, motor drive, active filter, electric vehicles, hybrid electric vehicles, naval/space/aerospace compact power conversion modules, uninterrupted power supplies and etc. The DC-AC converter in these applications are required to provide high gain with high power density and less component count (Abdullah et al., 2012; Castilla et al., 2009; Inoue and Akagi 2007; Mazumder and Rathore 2011; Min et al., 2009; Swaminathan and Lakshminarasamma 2018; Zhao et al., 2014). Size and cost of the uninterruptible power supply are very important. Since the dimensions of the uninterruptible power supply are determined by DC-AC inverter, it is necessary to make a small DC-AC inverter. The most important factor determining the dimensions and weight of the DC-AC inverter is the transformer (Bodur, 2011).

In low frequency transformers designed for commercial frequency, the weight and volume reduction can be achieved by using materials with high magnetic permeability in the core structure. On the other hand, since the frequency and transformer dimensions vary inversely, the frequency can be increased to reduce the size of the transformer. However, increasing the frequency does not causes the losses to increase (Alkul and Demirbaş 2019; Bouley, 2017; UPS Dünyası, 2016; Itoh et al., 2014). With the advances in material technology, materials with high magnetic permeability such as ferrite have been used in transformers. As a result of the use of high frequency transformers with power electronics converters, high energy transformations can be made from low volumes. In addition, working at high frequencies reduces the size of the filter elements. The DC-AC converters using high frequency transformers in Figure 1 are preferred in all areas of technology to reduce converter size and filter requirement (Alkul and Demirbaş 2019; Lotfi and Wilkowski 2001; Swaminathan and Lakshminarasamma 2018).

The advantages of high frequency transformers are as follows:

- Total volume and weight are small,

- Filter sizes are small,
- Input/Output frequencies may be different,
- Can be connected to different phase system,
- Reduces input harmonics,
- Provides voltage regulation,
- The warming problem is minimal,
- Makes the task of isolation.

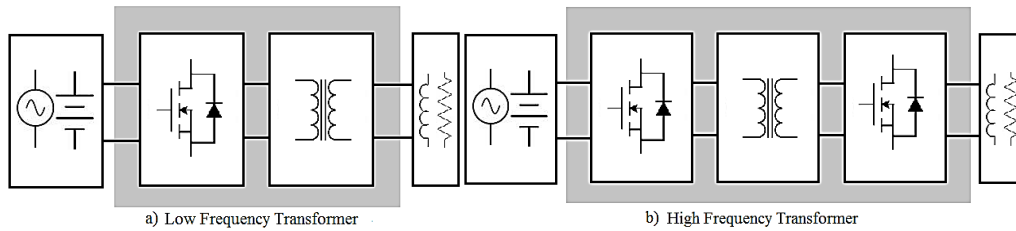


**Figure 1.** The DC-AC converters using low frequency and high frequency

In applications, high frequency transformer is used with two basic types of transducer structure. First, the input signal is converted to the alternate signal (Kjaer and Blaabjerg 2003; Nagao and Harada 1997; Papanikolaou et al., 2003). The second is applied to the high frequency transformer by converting the direct current voltage to alternating current voltage, the output voltage is rectified and the direct current signal is converted to the alternating current signal by means of a second converter (Alkul and Demirbaş 2019; Cacciato et al., 2010; Jung et al., 2002; Kjær, 2005; Lohner et al., 1996; Martins and Demonti 2001; Martins and Demonti 2002; Mekhilef et al., 2000).

Compared to conventional pulse width modulation converters with heavy and bulky line-frequency transformer, high-frequency transformer enables high frequency link power converters to offer high power density, compact size, and light weight (Zhu et al., 2014). Figure 2 (a) shows a conventional inverter solution diagram where the inverter uses conventional sine pulse width modulation scheme, Figure 2 (b) shows the solution diagram based on the principle of high frequency link inverter (Deng, et al., 2003; Muroyama et al., 1989; Yamato et al., 1988).

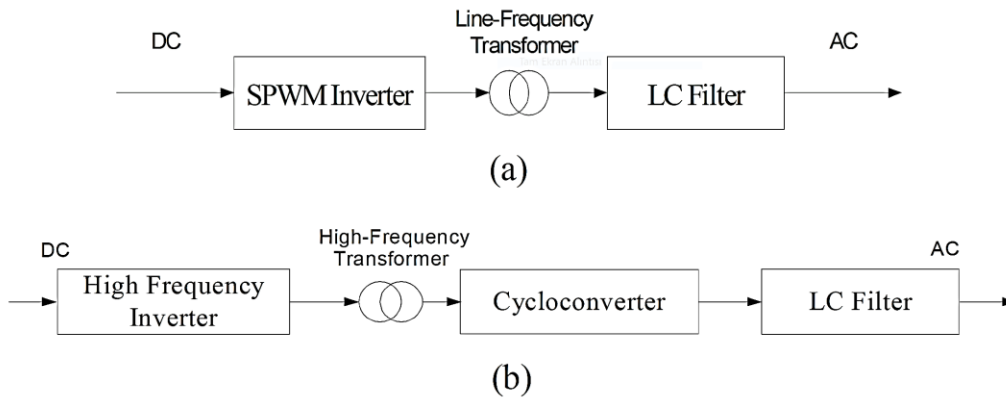


**Figure 2.** Block diagram representation of inverter solution

## 2. Materials and Methods

As shown in Figure 5, M1-M2 switches on the primary part of the circuit and M3-M4 switches on the secondary part of the circuit work ON and OFF in the ratio of 50%. The aforementioned switches on the primary and secondary parts work with a  $\Delta p.T$  phase difference. The frequency of the signal on the load is twice as much as that of the working frequency of the switches. The ratio of the positive alternate of the signal to its negative alternate depends on the  $\Delta p$  phase difference of the switches on the primary and secondary parts. The high frequency components in this signal are filtered out by the LC filter and at the output  $V_0$  voltage is acquired. And the transformer becomes smaller since it is switched at high frequency.

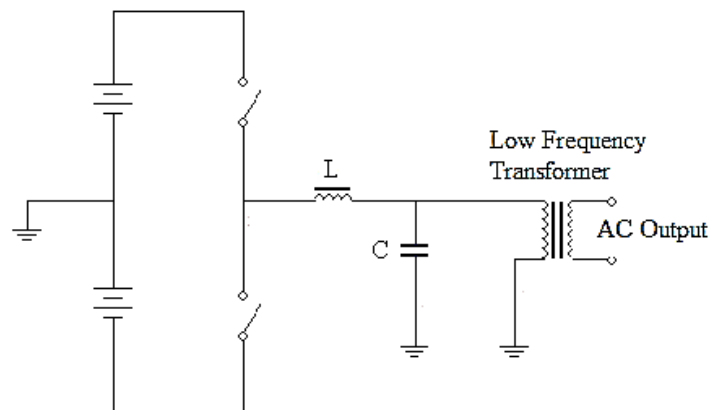


**Figure 3.** DC-AC inverter

In order to reduce the size of the DC-AC converter, the Pulse Width Modulation process with high frequency switching has been commonly used, as show in Figure 3. In this circuit, the LC filter becomes small enough by increasing the switching frequency and the transient response becomes quicker due to the miniaturized LC filter. However, the size of isolation transformer connected to the output is almost independent of the switching frequency, because the flux change in the transformer is mainly determined by the modulation signal of

the commercial AC line frequency of 50Hz and 60Hz. Therefore the high frequency switching in the converter does not contribute to reduce the size of the transformer (Harada et al., 1988).

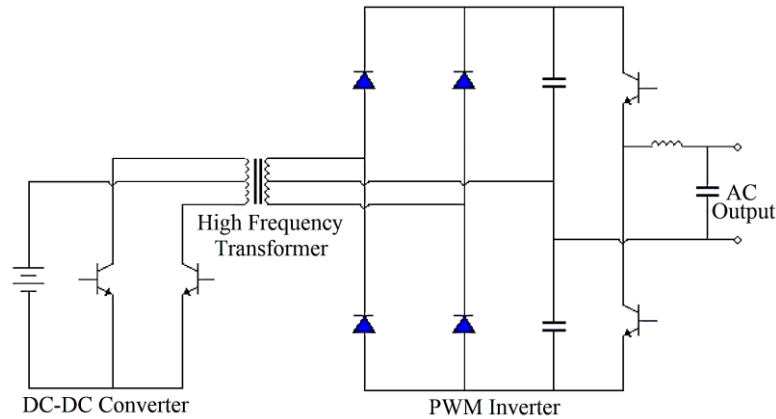


**Figure 4.** Pulse width modulation inverter with DC-DC converter

Figure 4 shows the case where the isolation is made in the from direct current to direct current converter followed by the Pulse Width Modulation inverter. The isolation transformer can be miniaturized by increasing the switching processes are necessary losses in such circuits are high and the reactive energy can not be recovered to the DC source through the DC-DC converter. The phase controlled DC-AC converter, which was originally presented by McMurray in 1970 is essentially suitable for making the isolation transformer small (McMurray, 1970). The original circuit, however, has the problem that the high current or high voltage surge may occur during commutation. This lessens the efficiency of the converter as well as the reliability of the system (Bodur, 2011).

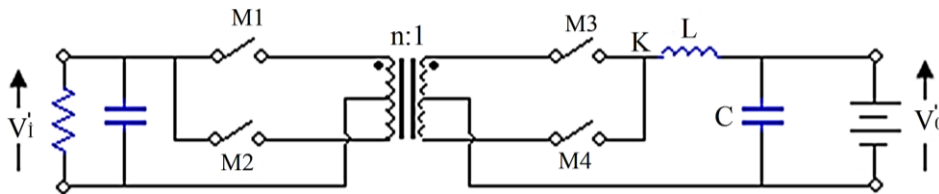


**Figure 5.** Basic diagram of phase controlled circuit.

As shown in Figure 5, M1 and M2 are alternatively driven with 50% duty ratio signals. If M3 and M4 are alternatively driven with other 50% duty ratio signals as shown in Figure 6 (a) and Figure 6 (b), the switch timing of M3 will delay from that of M1 by the period  $\Delta p.T$  (Harada et al., 1988; Deng et al., 2003; Chung et al., 1991).

In Figure 6 (c) is the Pulse Width Modulation voltage which appers at point K of Figure 5 When  $\Delta p$  is changed sinusoidally, the sinusoidal voltage  $V_o$  appers at the output terminal by removing the high frequency components with the LC filter (Harada et al., 1988).

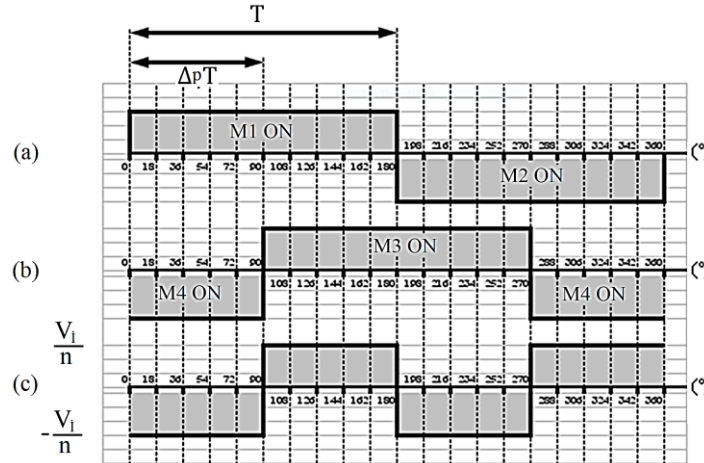


**Figure 6.** M3-M1, M4-M1 Phase difference and pulse width modulation

According to the state of the four switches M1-M4, the operation of the converter is classified into four states as shown in Figure 7 (I)-(IV). Among these four situation, which are repeated by turns, Figure 7 (I) and (III) are represented by the equivalent circuit as shown in Figure 8 (a), while Figure 7 (II) and (IV) are in Figure 8 (b).

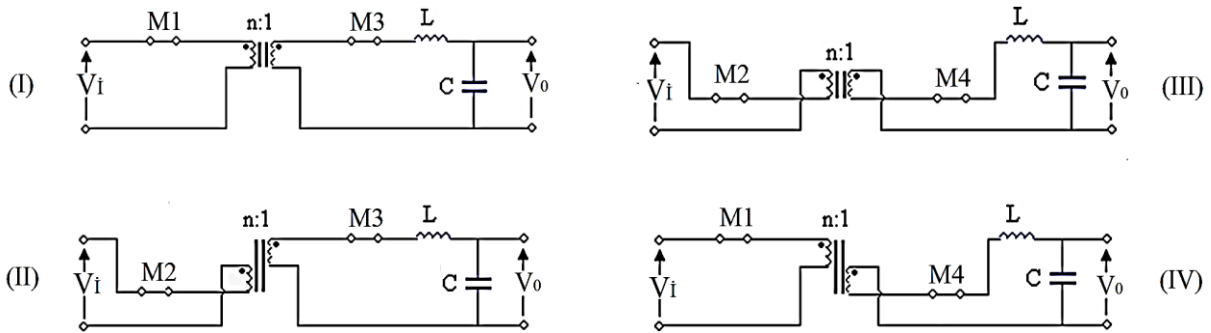


**Figure 7.** Operation phases of switches

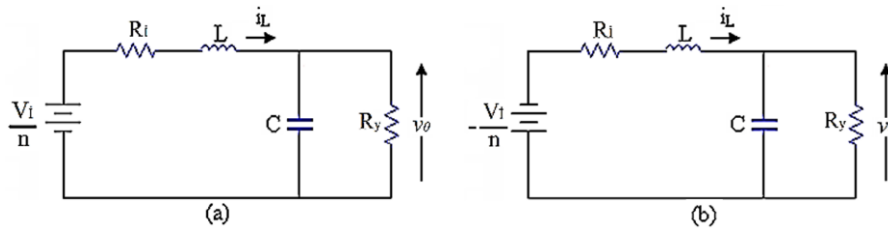


**Figure 8.** Equivalent circuits of operation phases

In Figure 8,  $R_i$  is the internal of the circuit and  $R_y$  is the load resistance. The winding ratio of the transformer is  $n$ .

On the practical assumption that the switching frequency ( $1/T$ ) is sufficiently higher than both the cutoff frequency on the LC filter and the modulation frequency, the output voltage  $V_0$  is derived like a buck type converter using the state space averaging method as follows (Harada et al., 1988; Middlebrook et al., 1976).

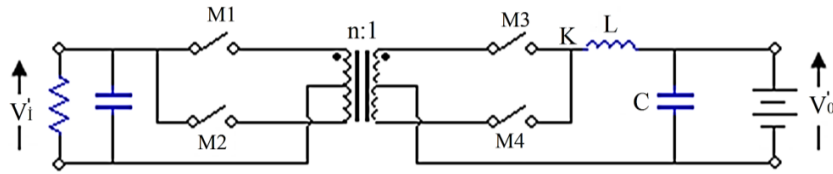


Figure 9. Phase controlled circuit

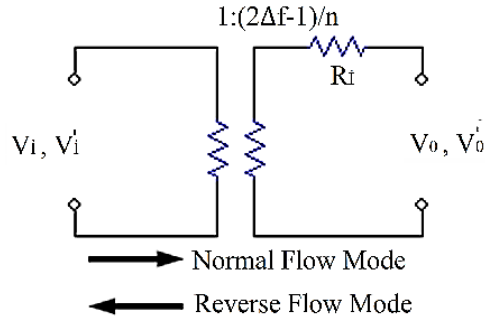


Figure 10. Averaged equivalent circuits

$$V_o = \frac{V_i (2\Delta_p - 1)}{n} \frac{1}{(1 + R_i/R_y)} \quad (1)$$

$$V_i' = \frac{n V_o'}{(2\Delta_p - 1)} \frac{1}{1 + (R_i n^2)/R_y' (2\Delta_p - 1)^2} \quad (2)$$

Figure 10 is the averaged equivalent circuit based on (1) and (2). It can be assumed that this equivalent circuit is 50Hz or 60Hz, because the frequency is sufficiently lower than the cutoff frequency of the LC filter. When the energy flows from the primary to the secondary of the transformer, the operation is called normal flow mode. On the other hand, when the energy flows from the secondary to the primary, the operation is called reverse flow mode. The equivalent turns ratio of the transformer is a function of the ratio  $\Delta_p$ , which is controlled by the modulation signal. If  $\Delta_p$  is changed sinusoidally with the center of 1/2, this circuit operates as a DC-AC converter. The power being able to flow bidirectionally through the equivalent DC transformer, the watt less power can be recovered to the primary source in the case of reactive load (Harada et al., 1988).

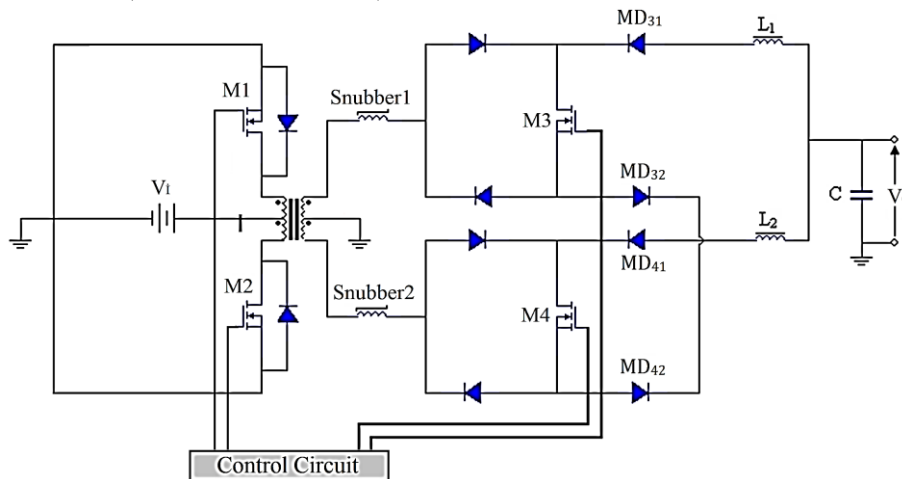
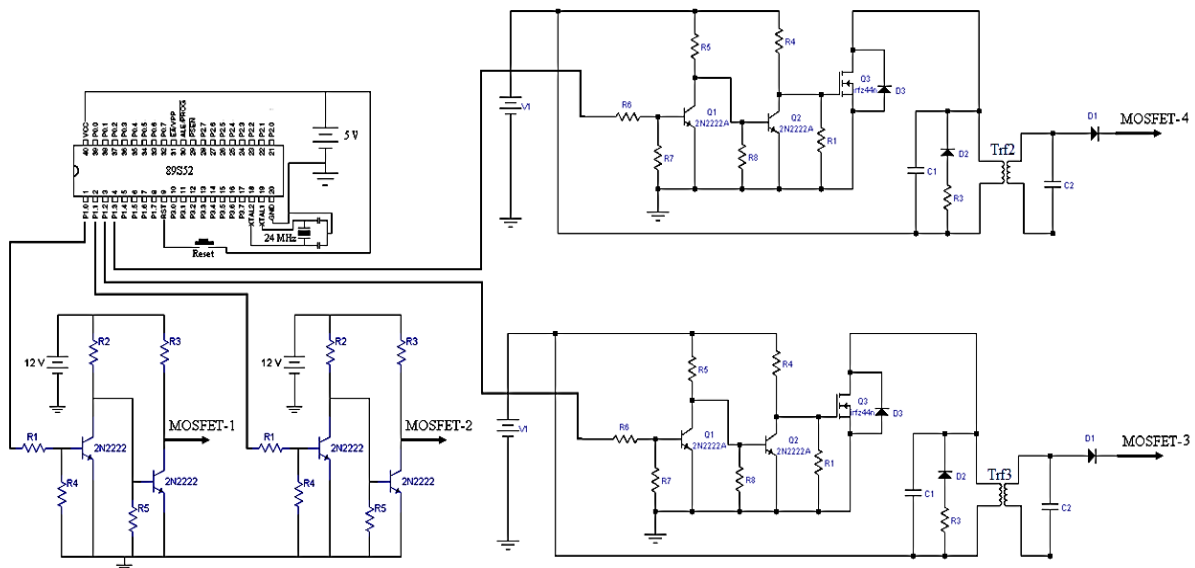


Figure 11. Scheme of the main circuit

The circuit of Figure 11, a pair of MOSFETs are used for the primary switches M1 and M2, and a pair of diode quads with a MOSFET are used for the secondary switches M3 and M4 so that the power may flow bidirectionally. The waveform of the driving voltage for MOSFETs is rectangular of 50 percent duty ratio, there is no DC bias in the driving transformers for MOSFETs. A high current surge or a high voltage surge is liable to occur during commutation between M3 and M4 for the following reasons. If the ON time of M3 and that of M4 overlap each other, the secondary winding of the transformer is short circuited by M3 and M4 to generate a high current surge. On the other hand, if there is a gap between the ON time of M3 and that of M4, a high voltage surge is impressed across the switching elements due to the stored energy in the reactor. This high current or high voltage surge lessens the efficiency of the converter and may cause serious damage to the switching elements. The solution to this problem is to divide the reactor into two parts, namely,  $L_1$  and  $L_2$  as shown in Figure 11. In this circuit, M3 and M4 are to be driven with a short overlap. Because the short current is blocked by the two reactors smooth commutation is realized in Figure 11, however, the small saturable reactors Snubber1 and Snubber2 are used as a magnetic snubber to suppress the switching current surge due to the excess charge in the diodes of MD<sub>31</sub>, MD<sub>32</sub>, MD<sub>41</sub>, and MD<sub>42</sub>, and due to the parasitic capacitance in the switching elements (Harada et al., 1988).

The  $\Delta p$  signal is generated in the control circuit. For this purpose, 89S52 microcontroller was used (Gümüşkaya, 2007). The supply of the  $V_{GS}$  voltages required to drive the M3 and M4 MOSFETs on the secondary side must be isolated. The trigger transformer can be used to drive MOSFETs, or it can be used in Opto-coupler. As shown in the circuit in Figure 12; By using Trf2 and Trf3 transformers, the signals in the secondary of these transformers are isolated from the main circuit. Thus, the drive signal required for the two MOSFETs in the secondary circuit can be obtained. In Figure 13, Opto-coupler was used to provide insulation. In this study, the transformer circuit is preferred while the analysis of the circuit is made with Opto-coupler, which takes less space and is easier to control in practice (Elmas, 2006).



**Figure 12.** Drive circuit using transformer.



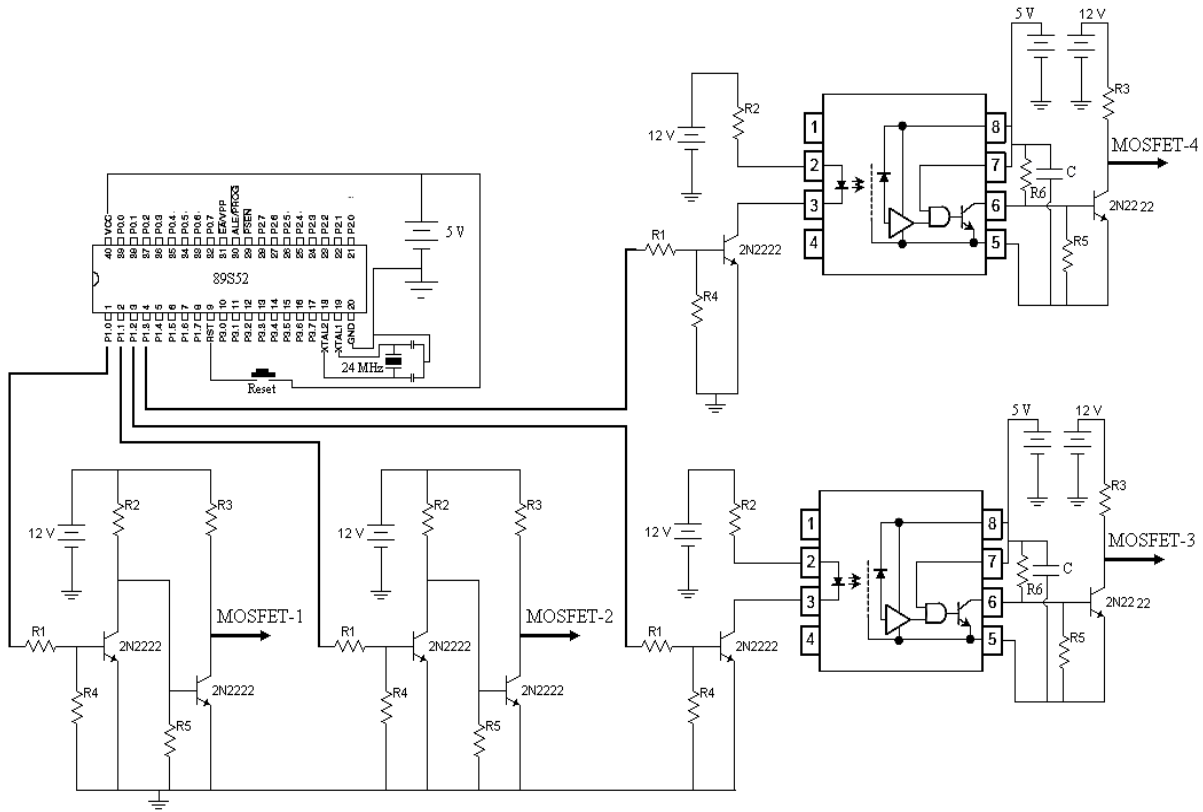


**Figure 13.** Drive circuit using opto-coupler.

89S52 from the 8051 Microcontroller family was used to drive the switch and create the required phase difference (Gümüşkaya, 2007; Topaloğlu et al., 2003). The phase difference between M1 and M3 is called  $\Delta_p$  and is calculated by the following method (Elmas, 2006).

$$\Delta_p = \frac{\text{Phase difference between M1 and M3}}{180} \quad (3)$$

In Table 1,  $V_0$  output voltage average values are given as a result of the changes in  $\Delta_p$ , and  $V_0$ - $\Delta_p$  graph is drawn by using these values in the table (Elmas, 2006).

### 3. Simulation and Experimental Evaluation

The high frequency switched phase control DC-AC inverter scheme that was followed through during the practice is shown at Figure 14. The M1 and M2 switches on the primary part of the transformer and the M3, M4 switches on the secondary part work ON and OFF in the ratio of 50% among each other. The switches in the primary and the secondary parts work according to the  $\Delta_p$  value that creates and controls the phase difference between the two.  $\Delta_p$  can be modified between zero and one according to the desire and the circumstances. The ratio of the positive alternate to the negative alternate of the voltage on the load depends on the  $\Delta_p$  value. The frequency of the signal that is on the load of the circuit is twice as much as the switch frequency and the voltage value depends on the transformation of the transformer (Elmas, 2006).

Since the signals of the microcontroller must be fortified in order to drive the MOSFET in the primary part with the microcontroller, a MOSFET driving circuit is designed with the use of two 2N2222 between the microcontroller and the MOSFET as can be observed in Figure 14. In order to drive the MOSFET in the secondary part with the signals coming from the microcontroller, besides fortifying the signal, the isolation of the  $V_{GS}$  voltage is necessary. For that purpose, a driving circuit where two 2N2222 and TLP 2061 opto-coupler for isolation is used. The high frequency transformer in the circuit is wound around an E-Core.

The diameter of the wire used for the primary windings of the transformer is 1mm and 15 windings were completed. The diameter of the wire used for the secondary windings of the transformer is 0,5 mm and 144 windings were completed. As a result, a high frequency transformer is designed which has six taps and whose transformation ratio is four. The input voltage of the circuit is 24 V and the output voltage is 220 V. Since the work is a prototype work, a 110 W DC-AC inverter is designed (Elmas, 2006).

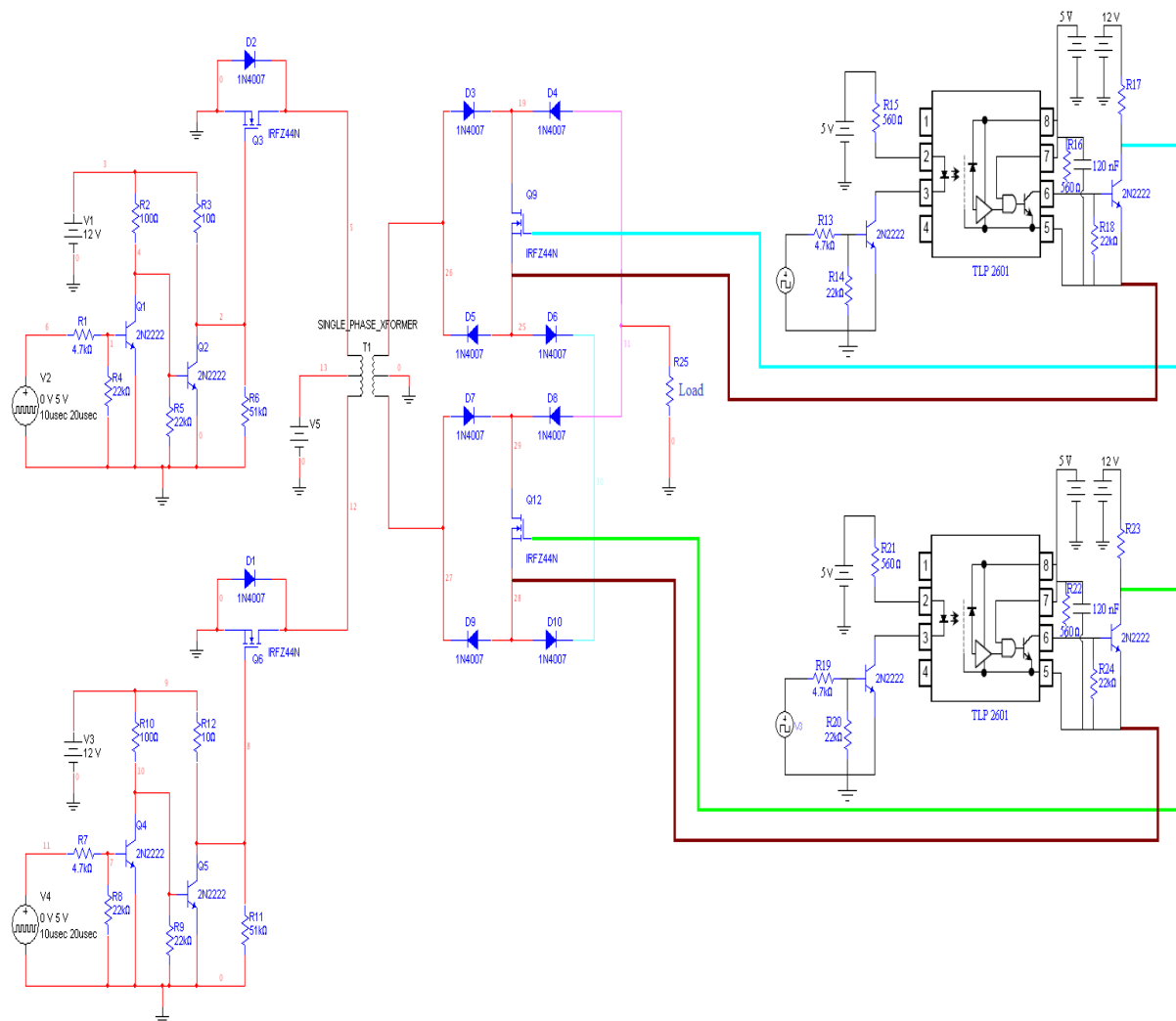


**Figure 14.** Main circuit diagram.

The  $\Delta p$  value was changed from 0.1 to 1 by 0.1 steps with the program written for the microcontroller. The average value of the output voltage for each value of  $\Delta p$  is given in Table 1 and at the Figure 15.

**Table 1.** M3-M1, M4-M1 Phase differences and average  $V_0$  (V)

$\Delta p$	M3-M1 Phase difference	M4-M1 Phase difference	Ort. $V_0$ (V)
0	0	180	-220
0.1	18	198	-176
0.2	36	216	-132
0.3	54	234	-88
0.4	72	252	-44
0.5	90	270	0
0.6	108	288	44
0.7	126	306	88
0.8	144	324	132
0.9	162	342	176
1	180	360	220

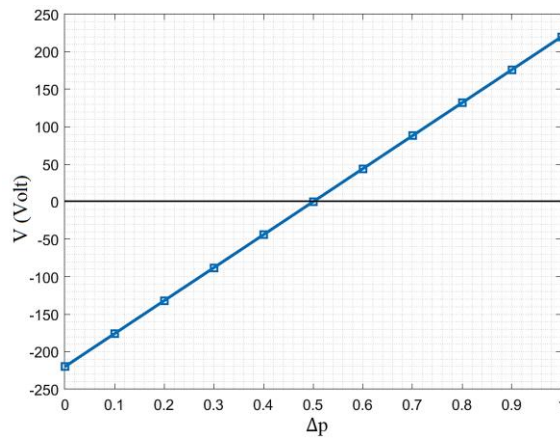


**Figure 15.**  $V_0$ - $\Delta p$  graph

The output signal of the circuit for  $\Delta p = 0.5$  is a square wave. The frequency of the signal is about 20 kHz. For commercial frequency, this signal is not suitable for an inverter output. As can be seen in Figure 15, when the  $\Delta p$  value is changed by 0.1 steps in the range of 0-1, the output signal is similar to the rising edge of a triangular wave. By setting the  $\Delta p$  value to the appropriate values with this method, a 50Hz triangular wave can be obtained as in Figure 16.

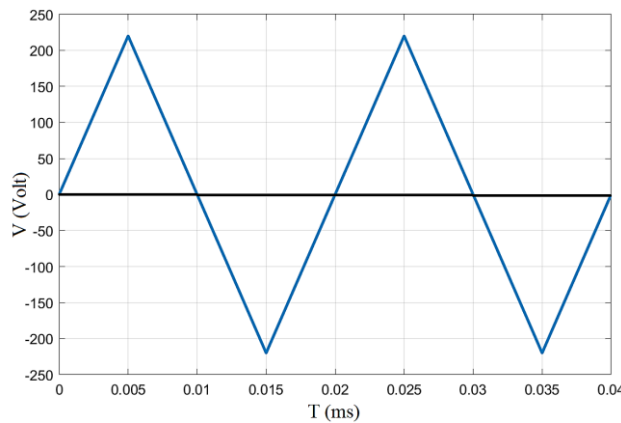


**Figure 16.** 50Hz triangular wave obtained from T values

With a similar method, a 50Hz sine signal can be obtained at the circuit output. Table 2 shows the  $\Delta p$  values obtained by adjusting the  $\Delta p$  values of the signal in Figure 16 and the sine values corresponding to these values. The circuit output signal obtained as a result of the switching applied with the program written to the microcontroller with these  $\Delta p$  values is as in Figure 17.

**Table 2.** Sine wave  $\Delta p$  values

Triangle Wave		Sine	
$\Delta p$	$V_0$ (Volt)	$\Delta p$	$V_0$ (Volt)
0.50	0	0.50	0
0.60	44	0.66	68
0.70	88	0.79	129
0.80	132	0.91	178
0.90	176	0.98	209
1.00	220	1.00	220
0.90	176	0.98	209
0.80	132	0.91	178
0.70	88	0.79	129
0.60	44	0.66	68
0.50	0	0.50	0
0.40	-44	0.35	-68
0.30	-88	0.21	-129
0.20	-132	0.10	-178
0.10	-176	0.03	-209
0.00	-220	0.00	-220
0.10	-176	0.03	-209
0.20	-132	0.10	-178
0.30	-88	0.21	-129
0.40	-44	0.35	-68
0.50	0	0.50	0

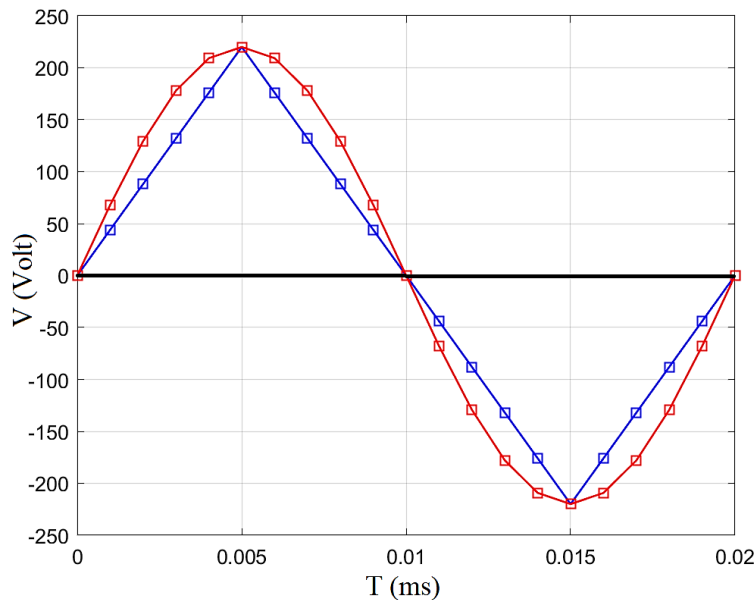


**Figure 17.** Triangle-Sine transformation

The pictures of the practice circuit are demonstrated in Figure 18. The circuit is loaded with 110 W. The output voltage of the circuit is 220 V, its efficiency is 93%.

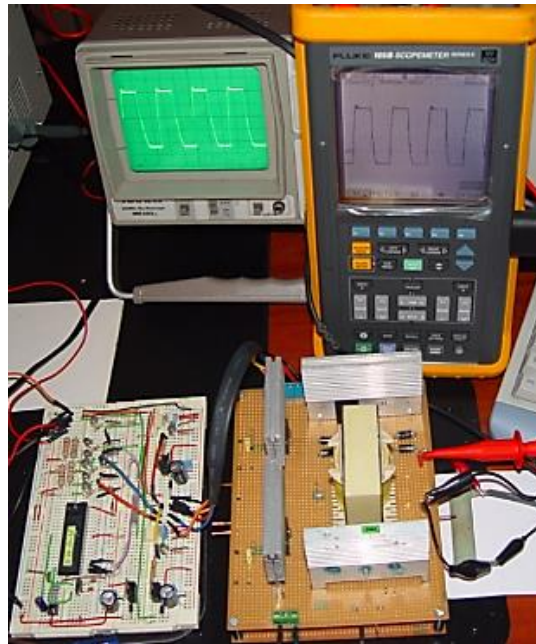


Figure 18. Application circuit

The graphs in Figure 19 are the Oscilloscope outputs obtained for  $\Delta p = 0,1$  values from the application circuit given in Figure 18.

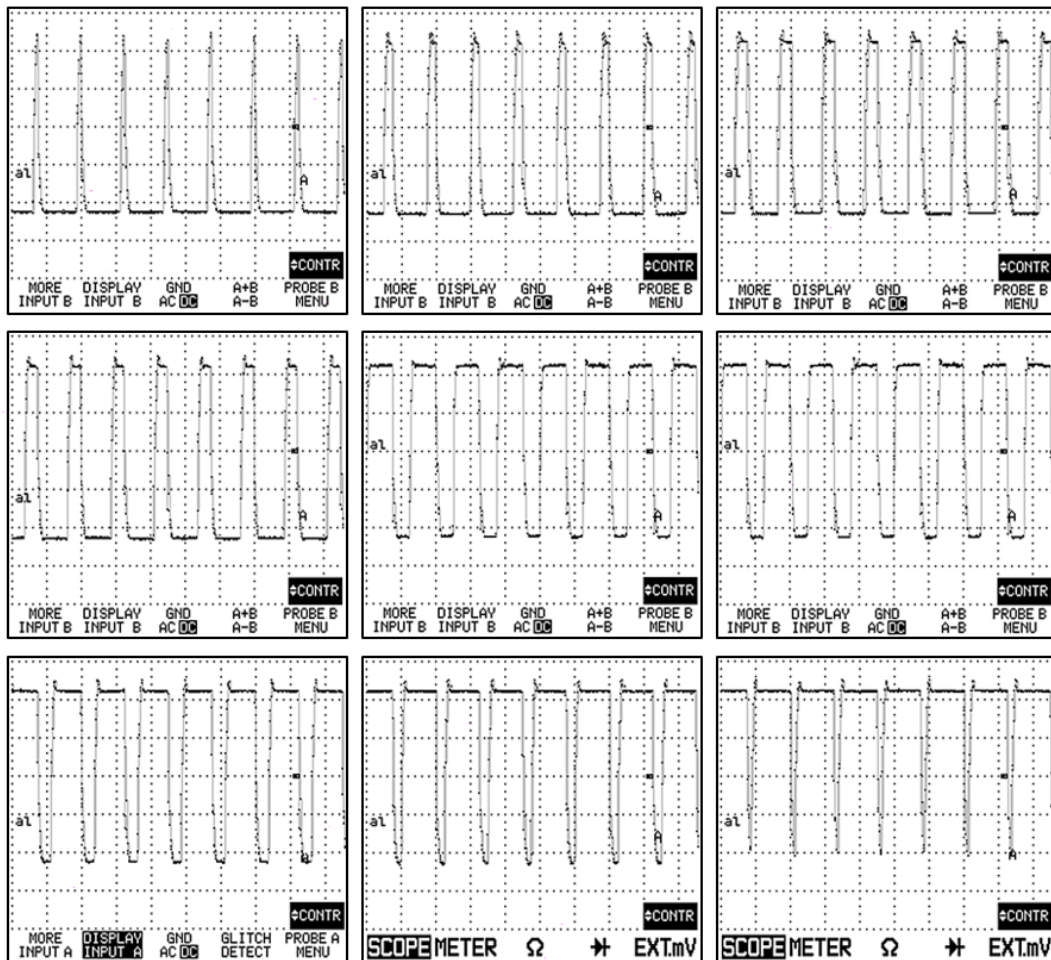


Figure 19. Voltage over load for  $\Delta p=0,1-0,9$  values in oscilloscope.

The microcontroller was programmed with the data in Table 2, and then switching was done with this microcontroller and 220 V sinus in Figure 20 was obtained.

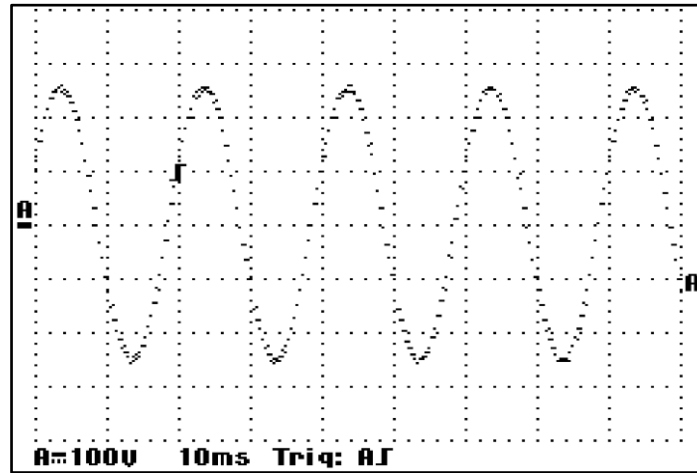


Figure 20. Circuit output signal

The data of the application circuit in Figure 18 is given in Table 3.

Table 3. Application circuit output

Application Circuit Data	
Input Power	118.27 W
Output Power	110 W
Input Voltage	24 V
Output Voltage	220 V
Switching Frequency	20 kHz-50 kHz
Efficiency	0.93

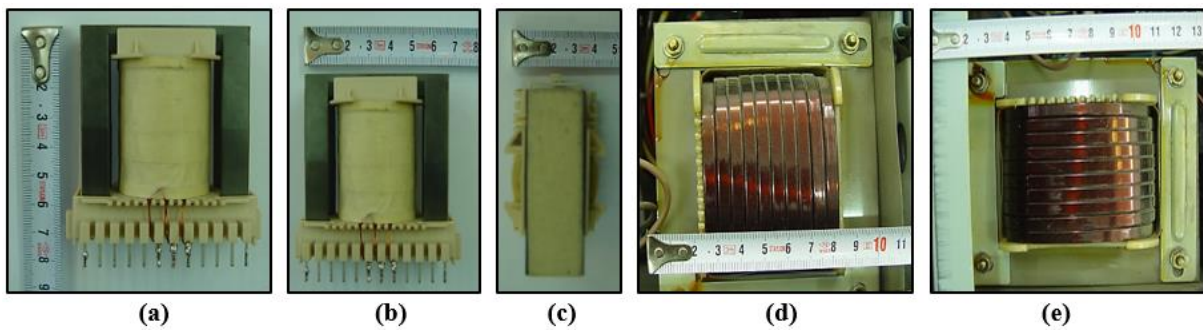


Figure 21. High frequency transformer with ferrite core and sheet metal core transformer.

In Figure 21 (a,b,c), the measurements of the ferrite cored transformer used during practice is demonstrated, and in Figure 21 (d,e) the measurements of a metal-plated transformer is demonstrated. The measurements of ferrite cored high frequency transformer are 7x6,5x4 cm, and the measurements of the metal plate cored transformer that has the same power are 13x10x10 cm. The ratio of the mass of the ferrite cored high frequency transformer that is switched at 20 kHz to the mass of the metal plate cored transformer is approximately 1/7. The ratio of the weight of the transformers is 1/10.

#### 4. Conclusions

The voltage transfer ratio of the circuit can be controlled with two couples of phase controlled switches. During the switching period, when the M3 and M4 switches in the secondary parts of the circuit are in transmission simultaneously, the secondary winding has short circuit. This condition causes the formation of high frequency waves. Additionally, if there is a gap in the increase and decrease switching period of M3 and M4, a high voltage wave occurs. Studies in the literature have similar current and voltage jumps. Faster MOSFET and diodes were used in this study. In addition, opto-coupler were used to switching MOSFETs on the secondary side of the circuit. This study, opto-coupler drive circuits were preferred to transformer drive circuits commonly used in the literature. This preference had made MOSFETs easier and faster switching. Thus, The increase and decrease of the MOSFET at the moments of transmission and cut had made simultaneous and thus the jumps caused by the current and the voltage are eliminated. As a result, a decrease in the productivity of the inverter and damage in the switches as a result of the voltage fluctuation had prevented. The ratio of the mass of the ferrite cored high frequency transformer that is switched at high frequency to the mass of the metal plate cored transformer is approximately 1/7. The ratio of the weight of the transformers is 1/10. When the size of the circuit with a high frequency transformer is taken into consideration with power source, driving circuits, switches, air conditioning fans and LC filters, it corresponds to 2/3 of the size of a circuit with metal plate cored transformer. Ratio of their weight is 1/5. Because the ferrite cored transformers are smaller, lighter and cheaper in comparison to the metal cored transformer, the high frequency switched DC-AC invertors, where ferrite cored transformers are used, are decided to be more suitable for uninterrupted power sources. Since the circuit was a prototype, high power was not used. The circuit is loaded with 110 W. The output voltage of the circuit is 220 V, switching frequency is 20 kHz, its efficiency is 93%. The same transformer can be used at 20 kHz 1000 W, at circuit 50 kHz 1600 W. In order to be able to signal at the desired period and amplitude at the circuit output,  $\Delta p$  value is set in the range of 0-1 and sent to MOSFET driver circuits in packets. Since the sine signal is obtained directly at the circuit output, no filter is designed for the circuit output. The size of this circuit had been reduced and the cost had been reduced.

#### Ethics in Publishing

There are no ethical issues regarding the publication of this study.

#### References

- Abdullah, M. F., Iqbal, S. and Masri, S. 2012. "A Novel Single Phase DC-AC Inverter". *IEEE Student Conference on Research and Development*. Electronic ISBN: 978-1-4673-5160-7.
- Alkul, O. ve Demirbaş, Ş. 2019. "Güç Elektroniği Transformatörlerinin İncelenmesi ve Bir DA/DA Dönüştürücü Uygulaması". *Gazi Üniversitesi, Fen Bilimleri Dergisi*. Part C, 7(2): 450-471.
- Bodur, H. 2010. Güç Elektroniği. *Birsen Yayınevi* (2017), ISBN-10: 9755115463



- Bouley, D. 2017. *Static or Rotary UPS: Which is Best for Your Application?* <https://blog.se.com/power-management-metering-monitoring-power-quality>. Erişim tarihi: 25.08.2021
- Cacciato, M., Consoli, A., Attanasio, R. and Gennaro, F. 2010. "Soft-switching converter with HF transformer for grid-connected photovoltaic systems". *IEEE Transactions on Industrial Electronics*, 57(5), 1678-1686.
- Castilla, M., Vicuña, L.G., Matas, J., Miret, J. and Vasquez, J.C. 2009. "A comparative study of sliding-mode control schemes for quantum series resonant inverters". *IEEE Trans. Ind. Electron.*, vol. 56, no. 9, pp. 3487–3495.
- Chung, Y.H., Shin, B.S. and Cho, G.H. 1991. Bilateral series resonant inverter for high frequency link UPS.
- Deng, S., Mao, H., Mazumdar J., Batarseh I. and Islam, K.K. 2003. "A new control scheme for high-frequency link inverter design". *Eighteenth Annual IEEE Applied Power Electronics Conference and Exposition*. 0-7803-7768-0/03/2003 IEEE 512.
- Elmas, B. 2006. *Yüksek frekans anahtarlamalı faz kontrollü DC-AC invertör*. Yüksek Lisans Tezi, Yıldız Teknik Üniversitesi, Fen Bilimleri Enstitüsü, İstanbul.
- Ferroxcube Databook. 2019. Soft Ferrites and Accessories, [www.ferroxcube.com](http://www.ferroxcube.com). Erişim tarihi: 10.09.2019.
- Gümüşkaya, H. 2007. Mikroişlemciler ve 8051 Ailesi. *Alfa Yayınları* (2007), ISBN: 9753160860
- Harada, K., Sakamoto, H. and Shoyama, M. 1988. "Phase-Controlled DC-AC Converter with High-Frequency Switching". *IEEE Transactions on Power Electronics*. Vol. 3. No. 4.
- Inoue, S. and Akagi, H. 2007. "A bidirectional dc/dc converter for an energy storage system with galvanic isolation". *IEEE Trans. Power Electron.* vol. 22, no. 6, pp. 2299–2306.
- Itoh, J., Oshima, R. and Takahashi, H. 2014. "Experimental Verification of High Frequency Link DC-AC Converter using Pulse Density Modulation at Secondary Matrix Converter". *IEEE International Power Electronics Conference*. Electronic ISBN: 978-1-4799-2705-0.
- Jung, Y., Yu, G., Choi, J. and Choi, J. 2002. "High-frequency DC link inverter for grid-connected photovoltaic system". In *Conference Record of the Twenty-Ninth IEEE Photovoltaic Specialists Conference*, 1410-1413.
- Kjær, S.B. 2005. *Design and control of an inverter for photovoltaic applications*. Institute of Energy Technology, Aalborg University.
- Kjaer, S.B. and Blaabjerg, F. 2003. "Design optimization of a single phase inverter for photovoltaic applications". In *IEEE 34th Annual Conference on Power Electronics Specialist*. PESC'03. Vol. 3, 1183-1190.
- Lohner, A., Meyer T. and Nagel A. 1996. "A new panel-integratable inverter concept for grid-connected photovoltaic systems". *IEEE proc. of the 1996 international symposium on industrial electronics (ISIE'96)*. Vol. 2, 827-831.
- Lotfi, A.W. and Wilkowski, M.A. 2001. "Issues and advances in high-frequency magnetics for switching power supplies". *Proceedings of the IEEE* 89.6, 833-845.
- Magnetics Databook. 2004. *Magnetics Catalog*, [www.mag-inc.com](http://www.mag-inc.com). Erişim tarihi: 25.08.2021.



- Martins, D.C. and Demonti, R. 2001. "Photovoltaic energy processing for utility connected system". In *IECON'01. 27th Annual Conference of the IEEE Industrial Electronics Society*. Cat. No. 37243. Vol. 3.
- Martins, D.C. and Demonti, R. 2002. "Grid connected PV system using two energy processing stages". In *Conference Record of the Twenty-Ninth IEEE Photovoltaic Specialists Conference*. 1649-1652.
- Mazumder, S.K. and Rathore, A.K. 2011. "Primary-Side-Converter-Assisted Soft-Switching Scheme for an AC/AC Converter in a Cycloconverter-Type High-Frequency-Link Inverter". *IEEE Transactions on Industrial Electronics*. Volume: 58, Issue: 9.
- Mcmurray, W. 1970. Power converter circuits having a high frequency link *U.S. Patent 3 517 300*.
- Mekhilef, S., Rahim, N.A., and Omar, A.M. 2000. "A new solar energy conversion scheme implemented using grid-tied single phase inverter". In *2000 TENCON Proceedings. Intelligent Systems and Technologies for the New Millennium*. Vol. 3, 524-527.
- Middlebrook, R.D. and Cuk, S. 1976. "A general unified approach to modeling switching converter power stages". *IEEE Power Electronics Specialists Conf. Rec.*, pp. 18-34.
- Min, B.D., Lee, J.P., Kim, J.H., Kim, T.J., Yoo, D.W. and Song, E.H. 2009. "A new topology with high efficiency throughout all load range for photovoltaic PCS". *IEEE Trans. Ind. Electron.*, vol. 56, no. 11, pp. 4427-4435.
- Muroyama, S., Aoki, T. and Yotsumoto, K. 1989. "A control method for a high-frequency link inverter using cycloconverter techniques". *Telecommunications Energy Conference, INTELEC '89, Conference Proceedings, Eleventh International.*, pp. 191-196, vol. 2.
- Nagao, M. and Harada, K. 1997. "Power flow of photovoltaic system using buck-boost PWM power inverter". In *Proceedings of Second International Conference on Power Electronics and Drive Systems*, Vol. 1, 144-149.
- Papanikolaou, N.P., Tatakis, E.C., Critsis, A. and Klimis, D. 2003. Simplified high frequency converter in decentralized grid-connected PV systems: a novel low-cost solution. In *proc. EPE'03*.
- Siemens Databook. 2019. Ferrites and Accessories, [www.epcos.com](http://www.epcos.com). Erişim tarihi: 25.08.2021.
- Swaminathan, N. and Lakshminarasamma, N. 2018. High Gain, High Frequency Link DC-AC Converter with Hybrid SPWM Scheme, *2018 IEEE International Conference on Power Electronics, Drives and Energy Systems (PEDES)*. Electronic ISBN: 978-1-5386-9316-2.
- TDK Databook. 2019. Ferrites for SMPS, [www.tdk.com](http://www.tdk.com). Erişim tarihi: 25.08.2021.
- Topaloğlu, N. ve Görgünoğlu, S. 2003. Mikroşlemciler ve Mikrodenetleyiciler. Seçkin Yayıncılık.
- UPS Dünyası. 2016. <http://www.upsdunyasi.com/ups-nedir.html> Erişim tarihi: 25.08.2021
- Yamato, I., Tokunaga, N., Matsuda, Y., Amano, H. and Suzuki, Y. 1988. "New conversion system for UPS using high-frequency link". *Power Electronics Specialists Conference, PESC '88 Record, 19th Annual IEEE*, pp. 658 -663 vol. 2.

- Zhao, B., Song, Q., Liu, W. and Sun, Y. 2014. "Overview of dual-activebridge isolated bidirectional DC-DC converter for high-frequency-link power-conversion system". *IEEE Trans. Power Electron.*, vol. 29, no. 8, pp. 4091–4106.
- Zhu, W., Zhou, K. and Cheng, M. 2014. "A Bidirectional High-Frequency-Link Single-phase Inverter: Modulation, Modeling, and Control". *IEEE Transactions on Power Electronics*. Volume: 29, Issue: 8.